Thin Digital Imaging Systems Using Focal Plane Coding

Andrew D. Portnoy[a], Nikos P. Pitsianis[a], David J. Brady[a], Jungpeng Guo[b],
Michael A. Fiddy[c], Michael R. Feldman[d], and Robert D. Te Kolste[d]

[a]Duke University Fitzpatrick Center for Photonics and Communication Systems and
Department of Electrical and Computer Engineering, Box 90291, Durham, NC 27708, USA;
[b]University of Alabama in Huntsville, 406 Optics Building, Huntsville, AL 35899, USA;
[c]University of North Carolina at Charlotte, 9201 Univ. City Blvd., Charlotte, NC 28223, USA;
[d]Digital Optics Corporation, 9815 David Taylor Dr., Charlotte, NC 28262, USA

ABSTRACT

With this work we show the use of focal plane coding to produce nondegenerate data between subapertures of an imaging system. Subaperture data is integrated to form a single high resolution image. Multiple apertures generate multiple copies of a scene on the detector plane. Placed in the image plane, the focal plane mask applies a unique code to each of these sub-images. Within each sub-image, each pixel is masked so that light from only certain optical pixels reaches the detector. Thus, each sub-image measures a different linear combination of optical pixels. Image reconstruction is achieved by inversion of the transformation performed by the imaging system. Registered detector pixels in each sub-image represent the magnitude of the projection of the same optical information onto different sampling vectors. Without a coding element, the imaging system would be limited by the spatial frequency response of the electronic detector pixel. The small mask features allow the imager to broaden this response and reconstruct higher spatial frequencies than a conventional coarsely sampling focal plane.

Keywords: Computational imaging, focal plane coding, multi-aperture imaging, super-resolution

1. INTRODUCTION

The Compressive Optical MONTAGE Photography Initiative (COMP-I) is an effort under the DARPA MONTAGE program to construct thin digital imaging systems while maintaining image quality metrics.[1] This paper presents the use of focal plane coding to produce nondegenerate data between subapertures of an imaging system.

The aperture size of a digital imaging system is determined by resolution and throughput specifications. In cases where resolution specifications may be satisfied by a small aperture one may choose to implement a "thin" digital imaging system with high throughput by using multiple apertures. This approach is taken, for example, the work of Tanida, et al., on TOMBO imaging systems.[2]

We construct an imager that generates these linearly independent codes using a binary, amplitude modulating focal plane mask. This coding element is fixed in contact with the imaging sensor in order to ensure placement in an image plane.

Multiple apertures generate multiple copies of a scene on the detector plane. The focal plane mask applies a unique code to each of these sub-images. Within each sub-image, each pixel is masked so that light from only certain optical pixels reaches the detector. Thus, each sub-image measures a different linear combination of optical pixels. This is possible here because the electronic pixels undersample the imaging system's optical resolution. By otpical pixels, we mean the minimum sized optically resolvable feature in the focal plane. Pixel mask coding has been used for coded aperture imaging in several instances.[3–9] An alternative focal plane code using a quantization of the discrete cosine transform is presented here.[10]

Further author information: (Send correspondence to D.J.B.)
D.J.B.: E-mail: David.Brady@duke.edu

Computational Imaging IV, edited by Charles A. Bouman, Eric L. Miller, Ilya Pollak,
Proc. of SPIE-IS&T Electronic Imaging, SPIE Vol. 6065, 60650F, © 2006 SPIE-IS&T · 0277-786X/06/$15

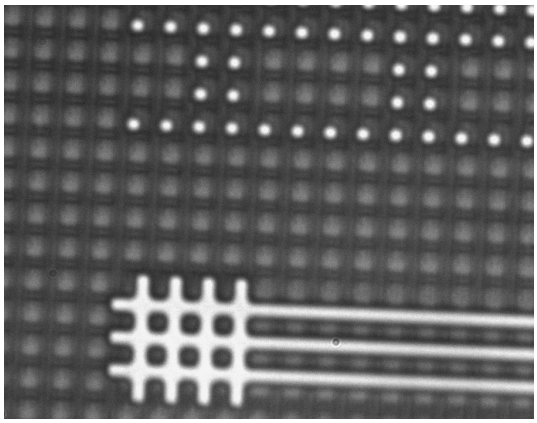

Figure 1. Microscope image of the imaging sensor with a focal plane coding element. The white dots and bars are alignment marks on the focal plane coding element.

Image reconstruction is performed by inversion of the linear transformation performed by the imaging system. Registered detector pixels in each sub-image represent the magnitude of the projection of the same optical information onto different sampling vectors.

Without a coding element, the imaging system would be limited by the spatial frequency response of the electronic detector pixel. The small mask features allow the imager to broaden this response and reconstruct higher spatial frequencies than a conventional coarsely sampling focal plane.

We present our latest developments in design of high resolution, thin imagers. It is important to realize that focal plane coding masks are simply one implementation of a coding scheme. A more ideal code may operate on a block of pixels rather than each pixel individually. Such a code would more evenly distribute information in an image with non-uniform information content. Future work will include incorporation of more complicated coding elements in order to perform more arbitrary transformations.

2. SYSTEM DESIGN AND COMPONENTS

2.1. Camera

A Lumenera Lu100 monochrome board level camera is used for data acquisition. The focal plane array is of size 1280x1024 pixels, each 5.2 μm x 5.2 μm. The imaging sensor, an Omnivision OV9121, is based on complementary metal-oxide semiconductor (CMOS) technology, where each pixel contains a photodiode and an individual charge to voltage circuitry. With current technology, these additional electronics reduce the light sensitive area of a pixel. In order to overcome this limitation, microlenses are fabricated over each pixel, improving quantum efficiency.

The manufacturer isolates the imaging sensor from the environment with a thin piece of glass. However, our experiments require that the focal plane coding element be placed in direct contact with the imaging sensor. Removal of the protective cover glass is required. It had been challenging to remove the glass with minimal damage to the underlying pixels. A procedure involving a chemical bath cocktail is used to dissolve the adhesive securing the cover class. An acetone and ethyl ether mixture was applied around the perimeter of the sensor. At the same time, a razor blade edge was used to scrape at and remove the residue of the adhesive. Multiple chemical applications have been necessary to completely free the cover glass.

2.2. Lenslet Array

The lenslet array used in the imager is a refractive/diffractive hybrid having two refractives and one diffractive per lenslet. The refractive lenses are fabricated using lithographic means on two separate 150mm wafers made of fused silica. The final lens shapes are aspheric. On the wafer surface opposite one of the lenses, an eight phase level diffractive is fabricated using the binary optics process. The diffractive primarily performs chromatic

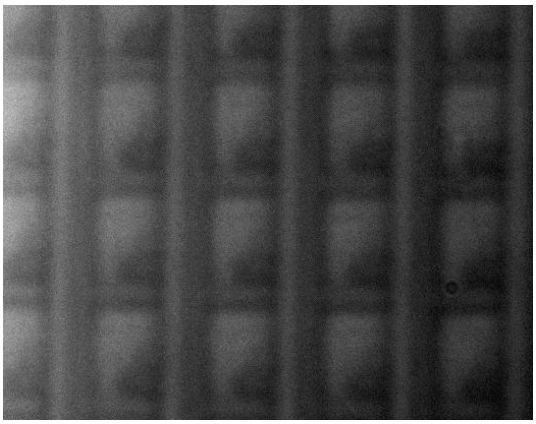

Figure 2. Microscope image of imaging sensor. The majority of the area of a pixel is a photo-diode. Charge to voltage electronics are visible in the lower right of each pixel.

aberration correction. The two wafers, one with refractives, and the other having refractives and diffractives, are bonded together, with the two refractive surfaces facing away from each other, via an epoxy bonding process. The gap between the wafers is controlled by a spacer layer of a patterned polymer, which has been spin-coated to a thickness of 20 μm and then patterned. After bonding, the wafer is singulated via a dicing process.

The completed optical system functions as an F/2.8 lens. It is designed to operate principally over the green portion of the visible spectrum, centered at 550nm. The limiting aperture is formed by a patterned chrome coating on the first surface of the optic, which is a refractive surface. In addition, an IR cut filter, in the form of a dielectric coating, is deposited on the first surface prior to the chrome deposition.

2.3. Focal Plane Coding Element

In order to improve upon an imager's resolution, by necessity, a focal plane coding element must contain subpixel features. In our system, we design a set of 16 unique square patterns to correspond with our 4×4 lenslet array. Every pixel in a given aperture is masked with the same pattern. We designate a central region of 1000×1000 pixels in our megapixel sized sensor as imaging pixels. Thus with a 4×4 lenslet array size, each of the 16 apertures correspond to a 250×250 pixel block. To recap, every pixel in a particular 250×250 block shares the same mask pattern, and this coding pattern differs from aperture to aperture.

The focal plane code corresponds to foldings of the shifted Hadamard matrix

$$S_{16} = \frac{1}{2}(H_{16} + 1)$$

where H_{16} denotes the Hadamard matrix of size 16. The focal plane code patterns are shown in Fig. 3. Black corresponds to 0 and denotes occlusion.

For our experiments, a binary coded pattern is employed, but one could also imagine a continuous design. Additionally, it is not necessary for each pixel in a given aperture to share the same mask pattern. This is merely done for simplicity.

Reduction lithography techniques are utilized to fabricate a patterned chrome layer on a thin glass substrate. In order to aid in the registration of the focal plane coding element with the pixel axis, the non-imaging perimeter pixels of the 1280×1024 sensor are used for alignment. Specifically, subpixel sized placement marks are patterned on the border outside the central 1000×1000 pixels on the glass substrate. These marks are visible under high power magnification.

We developed a special process in order to affix the glass substrate to the imaging sensor. A vacuum aids to hold the mask stationary while Newport AutoAlign positioning equipment with 100nm accuracy positioned the

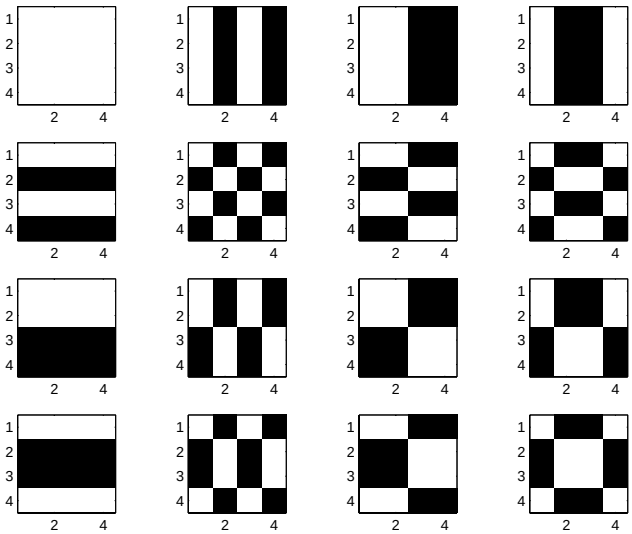

Figure 3. Focal plane code implemented in each aperture. Each figure is on the scale of a single pixel; the base feature size is one quarter pixel. All pixels in a given aperture share the same code.

camera board directly under the focal plane mask. Alignment is done to a first order ensuring that the mask completely resides within the active area of the imaging sensor. After the stages are also adjusted to minimize the gap between the glass and the detector, the vacuum is then turned off. With a small needle, a drop of UV curable adhesive is dispensed on the vertical edges of the glass. After sufficient time, capillary action draws a very thin layer of the viscous adhesive between the glass substrate and the imaging sensor. Images are gathered during this process to aid in the alignment of the pixels with the mask features. Using the positioning stages the mask is nudged very lightly with the tip of the adhesive distribution needle. When the mask is positioned in a desired location, a high intensity UV lamp is used to cure the adhesive.

3. LENS ALIGNMENT

A major challenge in the integration the system is the alignment of the lenslet element with the focal plane. With a focal length on the millimeter scale, the depth of focus for these lenses is on the order of micrometers. For such accuracy, bench top alignment methods are first employed to explore system performance. Computer aided design software is used to specify a custom lens mount for the lens wafer. The element is printed using a stereolithography machine. A 6-axis precision positioning system is used to adjust the camera board with respect to the stationary lens.

In order to align the focus, the lenslet array images a bright point source onto the detector. The source is placed on axis and in the far field at a distance of well over 100 focal lengths. One traditionally determines that a system is in focus when a point source in the object plane produces the most concise point spread function (PSF). In our system, the spatial extent of the PSF is smaller than a pixel. We claim that our system performance very nearly reaches the diffraction limit, with spot diameter equal to $2.44\lambda\frac{f}{d}$, where λ is the wavelength, f is the focal length and d is the lens diameter.

The challenge then becomes how to determine the best focus for the system when measurements are limited to the electronic down sampling of the optical field at resolutions equal to the pixel size. In order to attack this problem, sequential images are captured as the camera is translated along the optical axis. Qualitatively, when the image is out of focus, one observes light intensity spread over multiple pixels, and as the focal spot becomes smaller, the intensity becomes more localized to a single pixel. Numerically, one metric we employed is the calculation of the standard deviation of pixel value intensities in a cropped region surrounding the spot. When out of focus, one expects to see a lower standard deviation because of the more uniform distribution. If

the spot is in focus, though, and nearly all intensity is on a single pixel, the calculated standard deviation is much higher.

A potential complication is the possibility that the system is aligned in such a way that, when in best focus, an impulse falls centered on the border between 2 (or 4) pixels. The resulting captured image would still show intensity split between those pixels, even though the spot size is smaller than a single pixel.

However, the more interesting problem is determining the best focus for apertures with a focal plane coding element. If a point source is imaged to a masked region of the detector, one would expect to see minimal response when the system is in best focus. Furthermore, if the spot size grows, it could potentially increase the pixel response of a given camera, with minimal effect on neighboring pixels. Thus, the result would appear nearly identical to a situation where the system is in best focus imaging a point source to an unmasked region on the detector. In order to differentiate between the two, one needs to translate the image with respect to the camera pixels.

4. IMPULSE RESPONSE MEASUREMENT

The focal plane coding element modulates pixel responses differently in each aperture. Since the period of the mask pattern is equal to the pixel spacing, pixels in a given aperture all share identical modulation characteristics. However, calibration is needed to determine the exact registration of the mask with the camera pixels.

Impulse response measurements are taken at a variety of point source locations. Specifically, while translation stages positioned a point source perpendicular to the optical axis in a two dimensional grid, images are captured from the camera. A typical scan consists of 100x100 object locations covering approximately a 5x5 pixel square in image space. Thus, we are able to sample with subpixel positioning of the impulse on the detector. Essentially, we measure the convolution of the lens's PSF with the sampling function of the detector.

Data captured from two adjacent pixels in open aperture is shown in Fig. 4. As expected, there is only minimal variation between responses across apertures. The impulse response is shift invariant on a macro scale from pixel to pixel, but shift variant within a single pixel. The asymmetric nature of the pixel's sampling is most likely a result of the pixel's lack of sensitivity where the charge to voltage circuitry resides.

Even more interesting, though, is the modulation of the impulse response shown in Fig. 5 and Fig. 6. The focal plane coding element's effect is clearly visible. The pixel exhibits a narrow response due to the subpixel mask features. It is important to note again that a precondition of this result is that the PSF of the optical system is smaller than the features on the coding mask. Without such a well confined spot, the mask would not have such a significant effect. A larger spot would imply a narrower extent in the Fourier domain and would essentially low pass filter the aperture sampling function. An impulse response similar to that of the open aperture would be observed because the mask features (at higher spatial frequencies) would be attenuated.

5. RECONSTRUCTIONS

The image reconstruction consists of the following steps. First, the individual lenslet subimages are cropped from the sensor captured image. Then, the subimages are processed individually for noise removal and deconvolution of the corresponding lenslet distortions. Subsequently, relative intensity adjustments between the subimages are performed. Exact sub-pixels shifts are determined relative to the clear aperture subimage, and the subimages are realigned. Finally, the super-resolution image is reconstructed by combining and decoding the focal plane code of the subimages.

Details of preliminary sample reconstructions are shown in Fig. 7. The reconstructed image is compared to the upsampled –by linear interpolation– subimage from the clear aperture lenslet.

6. SUMMARY

A multiple aperture camera is created using a lenslet array and a standard focal plane array. Multiple downsampled images are captured simultaneously. To break the redundancy between images, a focal plane coding element is placed between the imaging sensor and the lenses. Because the electronic pixels undersample the optical field, this element is able to code each subimage uniquely. From the resulting measurements a single high resolution image is reconstructed from the mutliple lower resolution images.

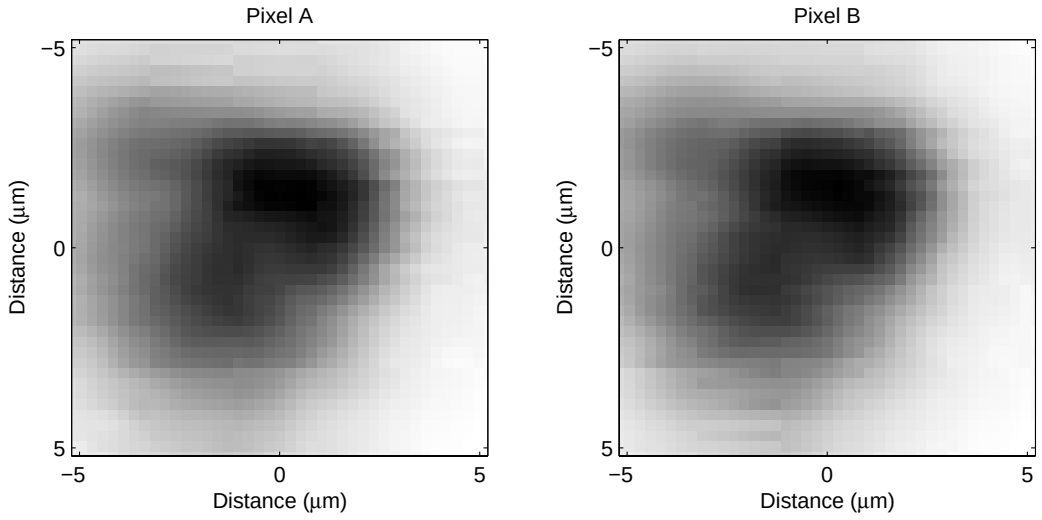

Figure 4. Impulse response for two adjacent pixels as a function of image location on detector plane.

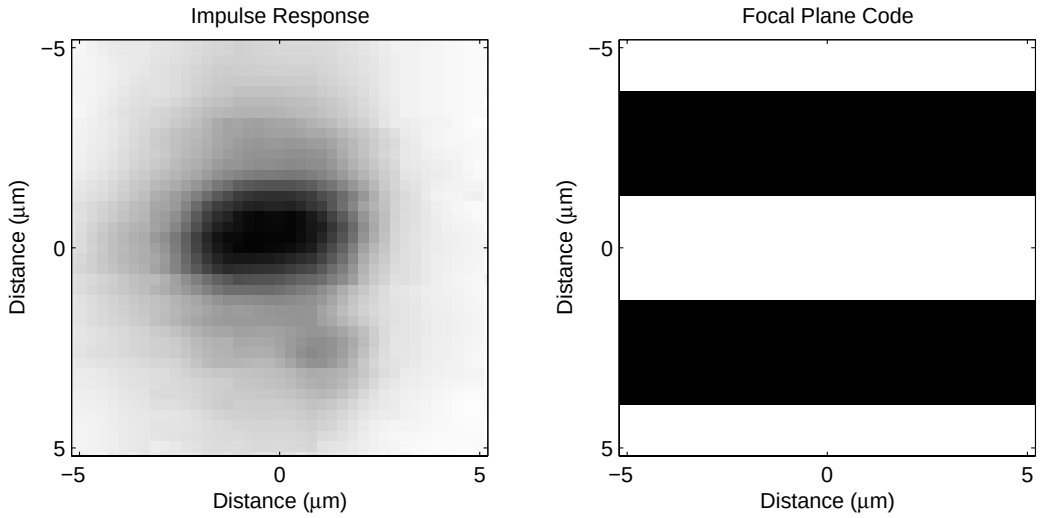

Figure 5. Impulse response of a pixel masked with a 50% horizontal grating with period equal to the pixel pitch.

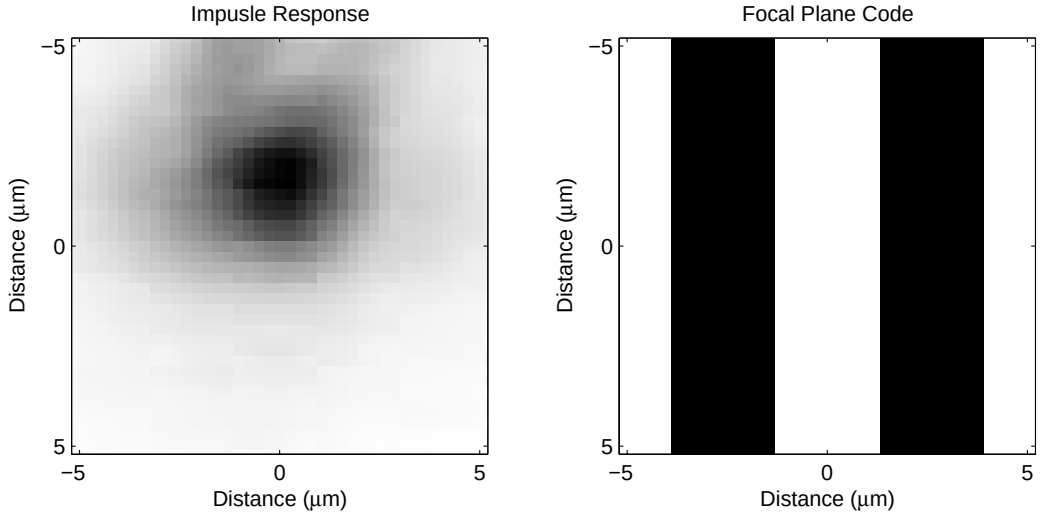

Figure 6. Impulse response of a pixel masked with a 50% vertical grating with period equal to the pixel pitch.

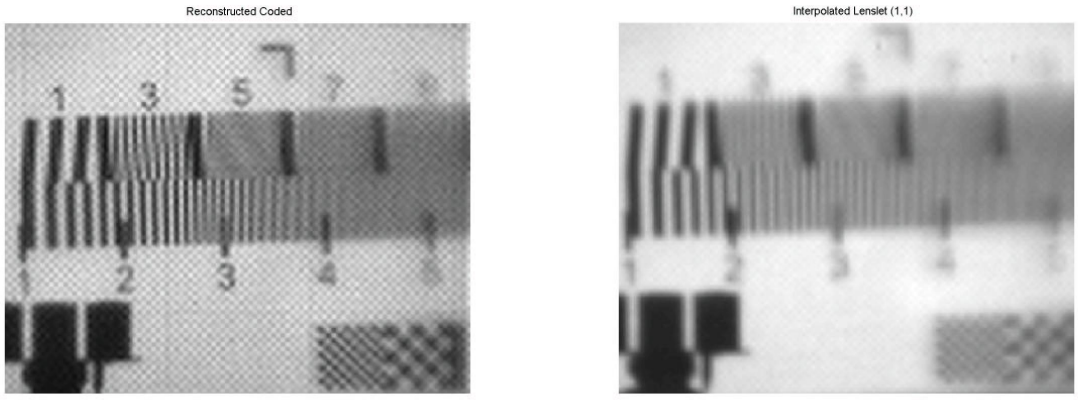

Figure 7. Details of the preliminary sample reconstructions (on the left), compared to interpolated upsamplings of the clear aperture image (on the right).

ACKNOWLEDGMENTS

This work was supported by the Defense Advanced Research Projects Agency (DARPA) under the Multiple Optical Non-redundant Aperture Generalized Sensors (MONTAGE) program.

REFERENCES

1. D. J. Brady, M. Feldman, N. Pitsianis, J. Guo, A. Portnoy, and M. Fiddy, "Compressive optical montage photography," in *Proc. SPIE, Photonic Devices and Algorithms for Computing VII;*, **5907**, pp. 52–58, 2005.
2. J. Tanida, T. Kumagai, K. Yamada, S. Miyatake, K. Ishida, T. Morimoto, N. Kondou, D. Miyazaki, and Y. Ichioka, "Thin observation module by bound optics (tombo): concept and experimental verification," *Applied Optics* **40(11)**, pp. 1806–1813, 2001.
3. E. E. Fenimore, "Coded aperture imaging - predicted performance of uniformly redundant arrays," *Applied Optics* **17**(22), pp. 3562–3570, 1978.
4. A. R. Gourlay and J. B. Stephen, "Geometric coded aperture masks," *Applied Optics* **22**(24), pp. 4042–4047, 1983.
5. G. Indebetouw and W. P. Shing, "Scanning optical reconstruction of coded aperture images," *Applied Physics B-Photophysics and Laser Chemistry* **27**(2), pp. 69–76, 1982.
6. M. Matsuoka and Y. Kohmura, "A new concept of x-ray microscopes with a coded-aperture imaging mask," *Japanese Journal of Applied Physics Part 1-Regular Papers Short Notes & Review Papers* **34**(1), pp. 372–373, 1995.
7. K. A. Nugent, "Coded aperture imaging - a fourier space analysis," *Applied Optics* **26**(3), pp. 563–569, 1987.
8. G. K. Skinner, "Imaging with coded-aperture masks," *Nuclear Instruments & Methods in Physics Research Section a- Accelerators Spectrometers Detectors and Associated Equipment* **221**(1), pp. 33–40, 1984.
9. R. F. Wagner, D. G. Brown, and C. E. Metz, "On the multiplex advantage of coded source aperture photon imaging," *Proceedings of the Society of Photo-Optical Instrumentation Engineers* **314**, pp. 72–76, 1981.
10. N. P. Pitsianis, D. J. Brady, and X. Sun, "Sensor-layer image compression based on the quantized cosine transform," in *Proc. SPIE, Visual Information Processing XIV*, **5817**, pp. 250–257, 2005.